

Tuning the Reactivity of a Cu/ZnO Nanocatalyst via Gas Phase Pressure

Luis Martínez-Suárez,¹ Johannes Frenzel,¹ Dominik Marx,¹ and Bernd Meyer^{1,2,*}

¹*Lehrstuhl für Theoretische Chemie, Ruhr-Universität Bochum, 44780 Bochum, Germany*

²*Interdisziplinäres Zentrum für Molekulare Materialien (ICMM) and Computer-Chemie-Centrum (CCC), Universität Erlangen-Nürnberg, 91052 Erlangen, Germany*

(Received 8 October 2012; published 20 February 2013)

By calculation of a thermodynamic phase diagram we provide an atomistic understanding of the morphological changes in ZnO-supported Cu nanocatalysts, which are subject to strong metal-support interactions, in response to the redox properties of the surrounding gas phase, i.e., depending on temperature and pressure. The reactivity, and thus the strong metal-support interactions, of this catalyst is traced back to a redox-state dependent occupation of delocalized ZnO substrate bands and localized Cu cluster states at the Fermi level. It is shown that at the conditions of industrial methanol synthesis complex electronic charge transfer processes across the metal-support interface, driven by morphological and electronic changes, explain the enhanced catalytic reactivity toward CO₂.

DOI: [10.1103/PhysRevLett.110.086108](https://doi.org/10.1103/PhysRevLett.110.086108)

PACS numbers: 68.35.Md, 68.43.Fg, 68.47.Jn, 73.20.At

Understanding structure-reactivity relationships and ultimately predicting reactivity is a key objective in fundamental research in heterogeneous catalysis. In many cases, however, the relevant catalytically active surface structures only evolve under the temperature and pressure conditions of the running chemical reaction. Oxide supported metal nanoparticles frequently display environment-driven morphological changes (so-called strong metal-support interactions [SMSI]) [1], which give rise to properties exclusive to the combined system and not present for the separate nanoparticles and metal oxide support. SMSI has been observed, in particular, for Cu nanoparticles dispersed on a ZnO matrix and stabilized by Al₂O₃ [2–4]. This nanostructured ternary compound is used in industry as an efficient and selective catalyst for the synthesis of methanol from syngas (CO, CO₂, and H₂) at about 520 K and 5–10 MPa [5]. The overall activity of the Cu/ZnO catalyst scales with the accessible Cu surface area [6]; however, bare Cu or Cu supported on other oxides is much less active than nanostructured Cu/ZnO, pinpointing to a SMSI-driven enhancement of the catalytic activity in Cu/ZnO with respect to bare Cu [3,6,7]. Rationalization of the nature of the SMSI is therefore a key element for understanding the catalytic activity of Cu/ZnO and many other supported catalysts.

Conflicting mechanisms have been proposed to rationalize the synergistic interaction between Cu and ZnO and the specific role of ZnO, as well as the nature of the active sites themselves. ZnO has been regarded as a reservoir for atomic hydrogen, which promotes H spillover to Cu [8], or as a matrix that stabilizes strain and planar defects in the nanosized Cu particles [4,9]. The increased catalytic performance of Cu/ZnO has been attributed to special active sites created by dynamic morphological changes of the Cu particles and a wetting of ZnO [2], by the decoration of the Cu particles with reduced ZnO [3,6], or by the formation of

a Cu-Zn surface alloy [7,10]. Finally, it has been suggested that electronic effects at the Cu/ZnO interface, in particular charge transfer from ZnO to Cu, promotes methanol formation from CO₂ [11,12]. Several of these effects may be relevant simultaneously, and their importance can change with catalyst preparation and environmental conditions. Concerning the general aim to obtain detailed knowledge of the relationship between atomic surface structure and catalytic activity, it has to be taken into account that the presence of a gas phase often drastically alters surface structure and oxidation state via temperature and partial pressure dependent adsorption [13]. Thus, catalytically active sites may be only created under reaction conditions, so that the catalytic activity is defined by the gas phase properties, as is most likely the case for catalysts showing SMSI.

Methanol synthesis on bare ZnO is a structure sensitive reaction [14], with the polar Tasker-type-3 ZnO surfaces [15] being most reactive [16]. Also in Cu/ZnO the polar ZnO surfaces show a much stronger material synergy with Cu than the other crystal facets [17]. Polar surfaces are particularly susceptible to reconstructions by loss of surface atoms and stabilization by adsorbates in order to become charge neutral [15]. The intimate interplay between temperature and pressure conditions of a surrounding gas phase and the most favorable mechanism to stabilize the polar ZnO surface was demonstrated by density functional theory (DFT) calculations [18,19]. DFT studies furthermore showed that the adhesion energy of Cu atoms, monolayers, and thin films on the polar ZnO surfaces strongly depends on the prevailing surface structure (whether surface bands are present or undercoordinated surface atoms have been saturated by adsorbates) determined by the gas phase environment [20]. Thus, the Cu-ZnO interaction strength and the redox properties of the surrounding gas phase are intimately coupled [20].

These studies provide us with the suitable background and methodologies to obtain an atomistic understanding of the structure and composition of Cu/ZnO catalyst surfaces that result from SMSI at the temperature and pressure conditions of industrial methanol synthesis. To be able to understand the enhanced reactivity of supported nanocatalysts that are subject to SMSI, we need to go beyond isolated metal clusters or low index metal surface models and include the response of the catalyst surfaces to changes in the gas phase environment. Based on a model system of a Cu_8 cluster supported on a polar O-terminated $\text{ZnO}(000\bar{1})$ surface we assess the relative energetics of a wealth of relevant phenomena, namely the ZnO reduction (via O vacancy creation and homolytic H adsorption) [19,21], the strength of the Cu-ZnO interaction at the interface [20], Cu adhesion in the cluster, reduced ZnO incorporation into the cluster, and Cu-Zn alloy formation. Employing DFT calculations to derive a thermodynamic surface phase diagram (see Supplemental Material [22]), we describe the morphology and oxidation state of our Cu/ZnO model surface as induced by the redox properties of the gas phase. The reactivity of the resulting structures is subsequently probed by calculation of the CO_2 adsorption strength, and the enhanced reactivity of Cu/ZnO under reducing conditions will be traced back to characteristic changes in the underlying electronic structure.

Figure 1 shows our calculated surface phase diagram of the thermodynamically most stable structures of the

Cu nanocatalyst supported on $\text{ZnO}(000\bar{1})$ as a function of O and H chemical potentials that reflect the composition, temperature, and partial pressure conditions of the surrounding gas phase. At moderate oxidizing and extreme H-poor conditions no hydrogen is present on the surface and the Cu_8 cluster wets the surface in a planar arrangement. Obviously, the interaction energy of Cu with the surface has become comparable to the Cu-Cu cohesion energy [20]. This occurs because under H-poor conditions Cu takes over the role of H to stabilize as much of the polar surface as possible. Increasing the H chemical potential, H atoms start to adsorb preferentially on the ZnO surface. As a result, the polar surface is stabilized by H and simultaneously Cu cohesion energy is gained by the formation of three-dimensional clusters comprising those Cu atoms that are no longer needed to saturate surface bonds. Similar H-driven morphology changes of supported metal nanoparticles were also reported for Pt and Pd clusters on Al_2O_3 [23]. At intermediate H chemical potentials the surface reaches a charge neutral, fully oxidized state and shows a band gap similar to the bulk. Both Cu and H contribute to the stabilization of the polar ZnO surface. The Cu cluster has obtained a compact, spherical shape in order to optimize its cohesion energy, whereas the Cu-free part of the surface is made charge neutral by H adsorption, for which in our specific example of a (4×4) surface unit cell and a Cu_8 cluster an H coverage of $1/4$ ML is needed. At higher H chemical potentials (> -1 eV) the ZnO surface gets

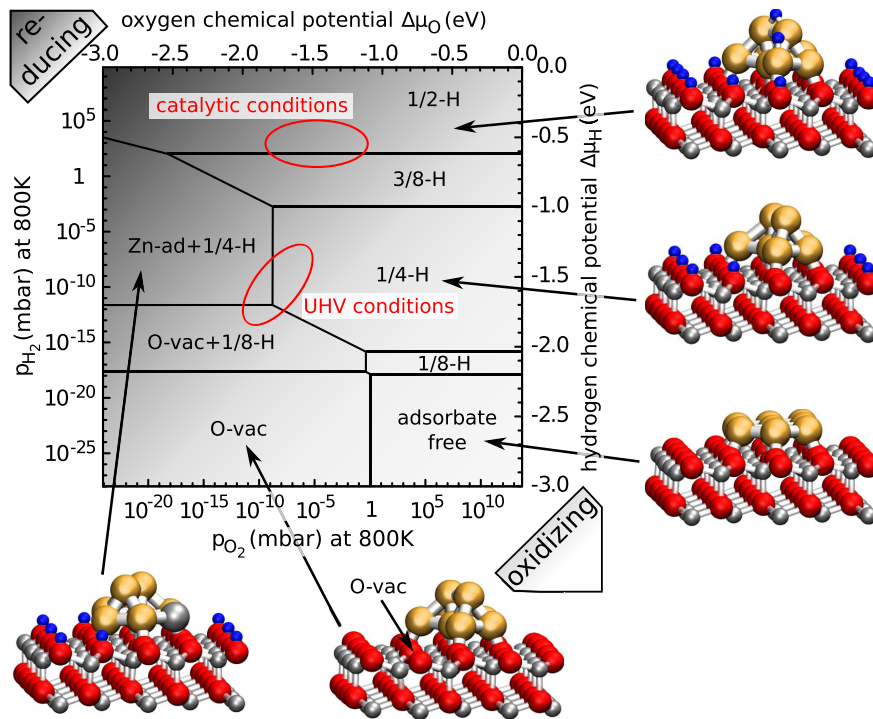


FIG. 1 (color online). Structural surface phase diagram of a Cu_8 cluster supported on a polar O-terminated $\text{ZnO}(000\bar{1})$ surface in thermodynamic equilibrium with O and H reservoirs controlling the chemical potentials $\Delta\mu_{\text{O}}$ and $\Delta\mu_{\text{H}}$. The lowest-energy surface structures are labeled according to their hydrogen coverage (x/y -H, in monolayers), Zn alloying (Zn-ad), or O vacancies (O-vac).

partially reduced by homolytic adsorption of additional H. The same behavior has been observed for the Cu-free surface [21]. Only above H chemical potentials of about -0.6 eV do H atoms start to adsorb on top of the Cu cluster where they are available for the methanol synthesis process.

Formation of O vacancies and H adsorption are competing processes for stabilizing the polar ZnO surface [19]. However, Fig. 1 shows that O vacancy formation only becomes the preferred mechanism at H- and O-poor conditions, similar to the bare ZnO surface without Cu [19]. With increasing H chemical potential at O-poor conditions, a mixture of O vacancies and adsorbed H becomes the preferred surface structure. Above $\Delta\mu_{\text{H}} = -1.7$ eV an interesting change occurs. Zn adatoms, another competing mechanism for achieving charge neutrality [19], become progressively more efficient in stabilizing the polar surface than O vacancies. This is due to an additional gain of cohesive energy caused by the integration Zn adatoms into the Cu cluster. Zn adatoms, therefore, do not appear on the Cu-free surface [19]. The most stable position of the Zn atoms is always directly at the Cu/ZnO boundary where the Zn atom is still incorporated in the cluster but can stabilize simultaneously a part of the polar surface next to it.

Altogether, we find that for temperature and pressure conditions of industrial methanol synthesis, Cu/ZnO is in a reduced state with homolytically adsorbed H on ZnO and additional H atoms on the Cu cluster, with an overall H coverage of about 1/2 ML. Under H-rich conditions the surface phase diagram in Fig. 1 nicely reflects the morphological structure and composition changes of ZnO supported Cu particles in response to the redox properties of the surrounding gas phase that have been proposed to explain the SMSI effect in Cu/ZnO catalysts [2–4]. Our DFT calculations demonstrate that these changes are driven by a rather subtle interplay between different mechanisms to stabilize the ZnO surface and to achieve charge neutrality, namely H adsorption, O vacancy formation, Zn adatoms, and Cu adhesion on the one hand, and the gain of cohesion energy by direct Cu-Cu and Cu-Zn interaction on the other hand. The balance of these energy contributions is already well captured by our Cu_8 cluster model (see Supplemental Material [22]).

The impact of the environment-driven morphology and composition changes on the reactivity of the Cu/ZnO catalyst surfaces can be seen by using CO_2 , the main carbon source in the methanol synthesis process [24], as a probe molecule. For three structures out of our phase diagram, Fig. 1, namely 1/2-H and 3/8-H as the thermodynamically most stable phases under catalytic conditions and Zn-ad+1/4-H representing a structure with Zn atoms migrated into the Cu cluster as observed by *in situ* spectroscopy [2], we investigated the full potential energy surface of the interaction of CO_2 with the Cu cluster and the ZnO surface.

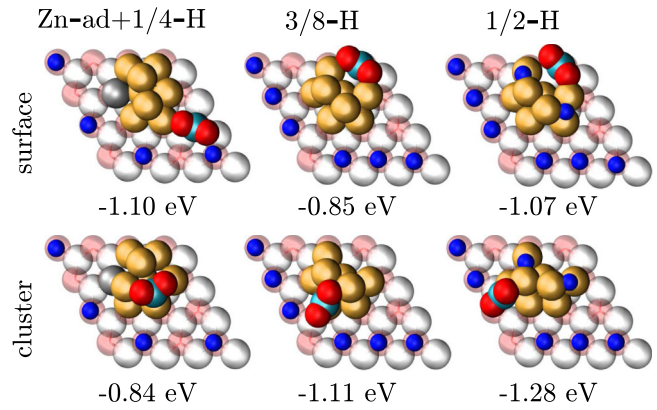


FIG. 2 (color online). Structures and adsorption energies of CO_2 for the most stable adsorption sites on the Cu cluster and the ZnO surface for the three surface models Zn-ad+1/4-H, 3/8-H and 1/2-H. Oxygen, zinc, hydrogen, and copper atoms are shown in red, grey, blue, and golden colors, respectively.

Surprisingly, we find that the global minima of adsorption for CO_2 (see Fig. 2) are rather insensitive to the redox state of the catalyst. The maximum binding energy for CO_2 only increases from 1.10 eV for Zn-ad+1/4-H to 1.28 eV in the 1/2-H model. However, the adsorption site changes notably. On 1/2-H and 3/8-H the binding of CO_2 to the Cu cluster is more favorable by about 0.2 eV compared to the adsorption on O sites of the ZnO surface, whereas for Zn-ad+1/4-H this trend is reversed. Upon adsorption on ZnO parts of the Cu/ZnO catalyst, CO_2 adopts a carbonate-like structure, similar to that on single-crystal ZnO surfaces [25]. In addition, the CO_2 binding energy is comparable [25]. However, the CO_2 molecules are also strongly activated when they adsorb on the Cu cluster and the CO_2 binding energy has become significantly larger than on single-crystal Cu surfaces [26] and unsupported Cu clusters [27].

The differences in the reactivity of the three surface models toward CO_2 can be rationalized by an examination of the electronic structure and the relevant electronic states. In the band structures of Fig. 3 we can distinguish between flat bands of localized states on the Cu cluster and dispersed ZnO bands of the substrate; however, some of them show a significant mixing of Cu-3d and O-2p orbitals of atoms sitting at the interface. Such mixed states with contributions on the cluster and the substrate can easily facilitate transfer of charge density across the cluster-substrate interface, which, concerning the reactivity, is especially interesting if these states are close to the Fermi level. The actual position of the Fermi level, on the other hand, depends on the reduction state of the surface, which, in turn, is determined by the redox properties of the gas phase.

For Zn-ad+1/4-H we find a very similar band structure as for charge neutral 1/4-H (not shown) with a clear band gap [see Fig. 3(b)]. The conduction band (CB) states of Zn-ad+1/4-H (marked as B1 and B2 in Fig. 3) play a

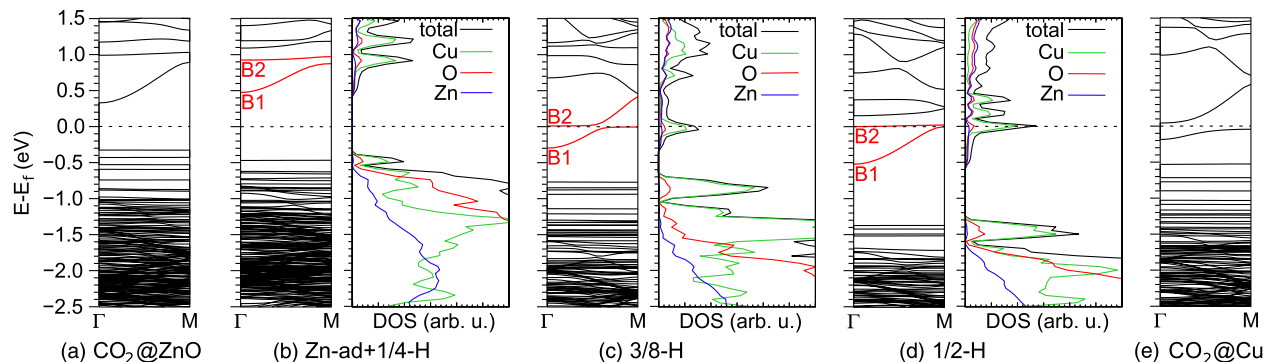


FIG. 3 (color online). Environment-dependent electronic band structures and species-resolved DOS. Catalyst structures are (b) Zn-ad+1/4-H (4 H on ZnO), (c) 3/8-H (6 H on ZnO), and (d) 1/2-H (6 H on ZnO and 2 H on Cu cluster). (a) and (e) indicate changes due to the site-specific adsorption of CO₂ on the ZnO surface of Zn-ad+1/4-H and on the Cu cluster of 1/2-H.

major role for the reactivity of the more reduced Cu/ZnO structures at higher H chemical potential. 3/8-H and 1/2-H have adsorbed successively one more H₂ molecule compared to 1/4-H: the first H₂ reduces the ZnO substrate and the second adsorbs on the Cu cluster, giving rise to two and four excess electrons, respectively. Figures 3(b)–3(d) show that the excess electrons start to occupy the lowest-lying CB of Zn-ad+1/4-H (the band B1), which becomes partially VB and CB in 3/8-H and filled VB in 1/2-H. Simultaneously, a flat band of localized copper states is lowered and gets partially occupied [see band B2 in Figs. 3(b)–3(d)].

The partial occupation of the B1 and B2 bands in 3/8-H and 1/2-H strongly enhances the reactivity of the Cu cluster to CO₂: both bands strongly mix with the CO₂ orbitals upon adsorption (see Supplemental Material [22]), resulting in a transfer of the excess charge to and an activation of the CO₂ molecule. This is in marked contrast to Zn-ad+1/4-H: B1 and B2 are empty and can not activate CO₂. Therefore, adsorption on the ZnO substrate and carbonate formation is preferred, which does not involve electronic states close to the Fermi energy. Thus, a reduction of the Cu/ZnO surfaces via adsorption of additional hydrogen enhances the reactivity of the Cu cluster over the reactivity of the ZnO substrate. Because the states of the B1 band, originally delocalized CB states of the ZnO substrate, have significant weight on the Cu cluster, an occupation of this band by reduction of the ZnO substrate pushes electrons into the Cu cluster. Simultaneously, a second band B2 of localized states on the Cu cluster becomes available to accommodate excess electrons after surface reduction. Indeed, direct experimental evidence for an enhancement of Cu/ZnO reactivity by electronic effects via an electron transfer from high-lying ZnO electronic states to the Cu Fermi level was recently reported by Liao *et al.* [12,17].

Our DFT calculations in conjunction with finite temperature and pressure thermodynamic analysis assemble a complex picture involving the interplay of redox state,

surface structure, and catalytic reactivity of both nano-dispersed Cu and ZnO support. A subtle interplay between ZnO surface stabilization via H adsorption, O vacancy creation, Zn adatoms, and Cu adhesion, as well as the gain of cohesion energy by direct Cu-Cu interaction together with Zn/Cu alloying, all depending on the redox properties of the environment and thus tunable via O and H gas phase chemical potentials, leads to a rich pattern of surface morphologies. Surface reactivity, in turn, depends on band filling and electronic charge transfer effects, which are controlled by the specific surface morphology that is generated at reaction conditions. At the temperature and pressure conditions of industrial methanol synthesis, excess H is adsorbed on the Cu cluster and the ZnO support, and the catalyst is in a reduced state. Under these H-rich conditions excess electrons in ZnO surface bands and partially filled, but previously unoccupied Cu states, increase the reactivity of the Cu cluster over that of the bare defective ZnO surface and create active sites for CO₂ chemisorption. We expect that these gas phase-induced complex changes in surface morphology and thus reactivity are not only fundamental to Cu/ZnO catalysts, but also of broad significance to heterogeneous catalysis of nano-dispersed metal/oxide-based catalysts in general.

This work was supported by the German Research Foundation (DFG) via Collaborative Research Center SFB 558 (Bochum) and the Clusters of Excellence RESOLV (EXC 1069, Bochum) and EAM (EXC 315, Erlangen), as well as by RD IFSC (Bochum). Computational resources were provided by BOVILAB@RUB (Bochum), RV-NRW and HLRB-II/SuperMUC.

*bernd.meyer@chemie.uni-erlangen.de

- [1] S. J. Tauster, S. C. Fung, R. T. K. Baker, and J. A. Horsley, *Science* **211**, 1121 (1981).
- [2] B. S. Clausen, J. Schiøtz, L. Gråbæk, C. V. Ovesen, K. W. Jacobsen, J. K. Nørskov, and H. Topsøe, *Top. Catal.* **1**, 367 (1994).

- [3] H. Wilmer and O. Hinrichsen, *Catal. Lett.* **82**, 117 (2002).
- [4] J. B. Wagner, P. L. Hansen, A. M. Molenbroek, H. Topsøe, B. S. Clausen, and S. Helveg, *J. Phys. Chem. B* **107**, 7753 (2003).
- [5] I. Chorkendorff and J. W. Niemantsverdriet, *Concepts of Modern Catalysis and Kinetics* (Wiley-VCH, New York, 2007).
- [6] M. Kurtz *et al.*, *Catal. Lett.* **92**, 49 (2004).
- [7] N.-Y. Topsøe and H. Topsøe, *Top. Catal.* **8**, 267 (1999).
- [8] M. S. Spencer, *Catal. Lett.* **50**, 37 (1998).
- [9] M. M. Günter, T. Ressler, B. Bems, C. Büscher, T. Genger, O. Hinrichsen, M. Muhler, and R. Schlögl, *Catal. Lett.* **71**, 37 (2001).
- [10] T. Fujitani and J. Nakamura, *Catal. Lett.* **56**, 119 (1998).
- [11] J. C. Frost, *Nature (London)* **334**, 577 (1988).
- [12] F. Liao, Z. Zeng, C. Eley, Q. Lu, X. Hong, and S. C. E. Tsang, *Angew. Chem., Int. Ed. Engl.* **51**, 5832 (2012).
- [13] P. Sautet and F. Cinquini, *Chem. Cat. Chem.* **2**, 636 (2010).
- [14] H. Wilmer *et al.*, *Phys. Chem. Chem. Phys.* **5**, 4736 (2003).
- [15] P. W. Tasker, *J. Phys. C* **12**, 4977 (1979).
- [16] J. Strunk, K. Kähler, X. Xia, and M. Muhler, *Surf. Sci.* **603**, 1776 (2009).
- [17] F. Liao, Y. Huang, J. Ge, W. Zheng, K. Tedsree, P. Collier, X. Hong, and S. C. Tsang, *Angew. Chem., Int. Ed. Engl.* **50**, 2162 (2011).
- [18] G. Kresse, O. Dulub, and U. Diebold, *Phys. Rev. B* **68**, 245409 (2003).
- [19] B. Meyer, *Phys. Rev. B* **69**, 045416 (2004).
- [20] B. Meyer and D. Marx, *Phys. Rev. B* **69**, 235420 (2004).
- [21] J. Kiss, A. Witt, B. Meyer, and D. Marx, *J. Chem. Phys.* **130**, 184706 (2009).
- [22] See Supplemental Material at <http://link.aps.org/supplemental/10.1103/PhysRevLett.110.086108> for details on the computational method, an estimate of cluster size effects, and plots of charge density distributions.
- [23] C. H. Hu, C. Chizallet, C. Mager-Maury, M. Corral-Valero, P. Sautet, H. Toulhoat, and P. Raybaud, *J. Catal.* **274**, 99 (2010).
- [24] G. C. Chinchin, P. J. Denny, D. G. Parker, M. S. Spencer, and D. A. Whan, *Appl. Catal.* **30**, 333 (1987).
- [25] Y. Wang *et al.*, *Angew. Chem., Int. Ed. Engl.* **46**, 5624 (2007).
- [26] L. C. Grabow and M. Mavrikakis, *ACS Catal.* **1**, 365 (2011).
- [27] Y. Yang, J. Evans, J. A. Rodriguez, M. G. White, and P. Liu, *Phys. Chem. Chem. Phys.* **12**, 9909 (2010).